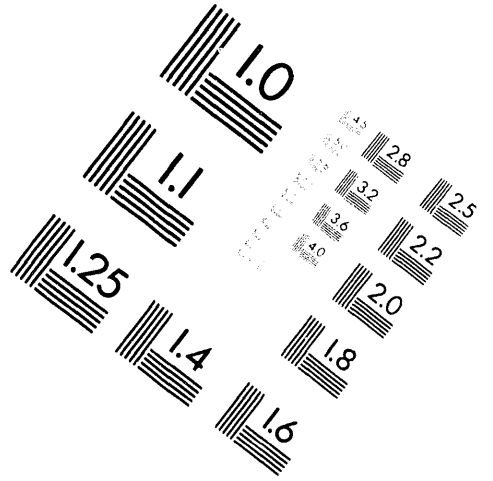
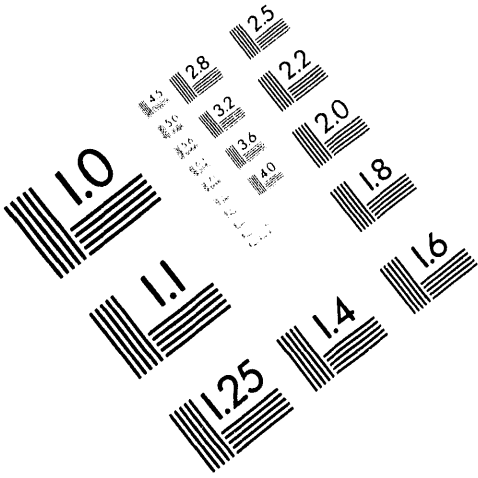




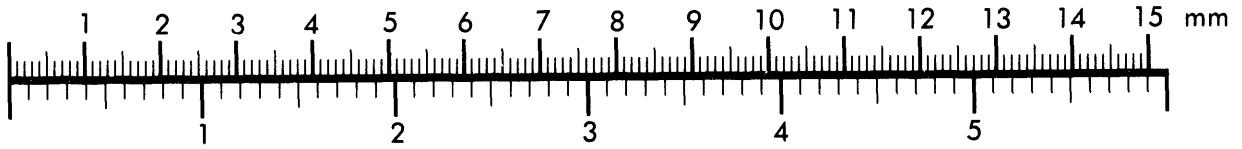
AIM

Association for Information and Image Management

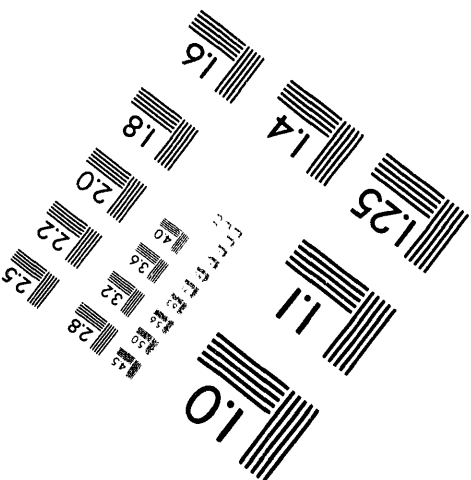
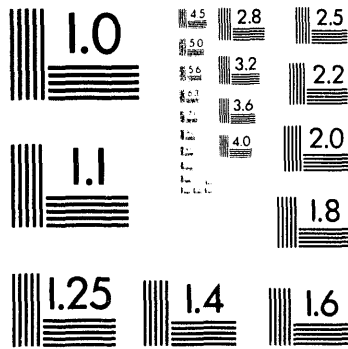
1100 Wayne Avenue, Suite 1100
Silver Spring, Maryland 20910
301/587-8202



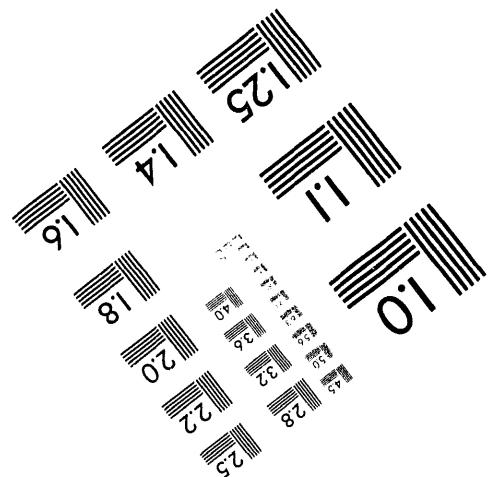
Centimeter



Inches



MANUFACTURED TO AIM STANDARDS
BY APPLIED IMAGE, INC.



1 of 1

Injection and Capture Simulations for a High Intensity Proton Synchrotron*

Conf-940618--12

Y. Cho, E. Lessner, K. Symon†

Argonne National Laboratory, 9700 Cass Ave., Argonne, IL 60439, USA

Abstract

The injection and capture processes in a high intensity, rapid cycling, proton synchrotron are simulated by numerical integration. The equations of motion suitable for rapid numerical simulation are derived so as to maintain symplecticity and second-order accuracy. By careful book-keeping, we can, for each particle that is lost, determine its initial phase space coordinates. We use this information as a guide for different injection schemes and rf voltage programming, so that a minimum of particle losses and dilution are attained.

A fairly accurate estimate of the space charge fields is required, as they influence considerably the particle distribution and reduce the capture efficiency. Since the beam is represented by a relatively coarse ensemble of macro particles, we study several methods of reducing the statistical fluctuations while retaining the fine structure (high intensity modulations) of the beam distribution. A pre-smoothing of the data is accomplished by the cloud-in-cell method.

The program is checked by making sure that it gives correct answers in the absence of space charge, and that it reproduces the negative mass instability properly. Results of simulations for stationary distributions are compared to their analytical predictions.

The capture efficiency for the rapid-cycling synchrotron is analyzed with respect to variations in the injected beam energy spread, bunch length, and rf programming.

1 INTRODUCTION

Feasibility studies for a one-megawatt spallation source have been undertaken at Argonne. The machine is designed to accelerate a high intensity proton beam from 400 MeV to 2 GeV, delivering 1.0×10^{14} protons at a repetition rate of 30 Hz. The ring magnet system is energized by a 20-Hz resonant circuit and de-energized by a 60-Hz resonant circuit, in order to reduce rf voltage requirements during acceleration. The 189-meter-long lattice has three long dispersion-free straight sections, and is composed of FODO cells with 90° phase advance per cell. A detailed description of the conceptual design of the machine is presented in [1].

One of the features of the synchrotron is to have negligible beam losses ($< 0.1\%$) during injection, acceleration,

and extraction. This goal is made more difficult by the presence of strong space charge effects due to the high beam intensity and relatively low injection energy. The space charge self-field can be very large and the available stable bucket area greatly reduced in comparison with the bucket area in the absence of space charge for identical kinematical parameters.

We have examined the effects on the capture efficiency of various parameters such as rf voltage programming, initial phase space distribution of the injected particles, and chopping of the linac beam to produce a shorter bunch.

In Section 2 we present the tracking program used in the simulations and the tests performed to validate its accuracy. In Section 3 we present an analysis of the capture efficiency for several initial conditions.

2 TRACKING PROGRAM

2.1 The Algorithm

The equations of motion are derived in Hamiltonian form suitable for numerical simulation [2]. The difference equations are implemented by a "leap-frog" algorithm and are accurate to the second order:

$$W_{n+1/2} = W_{n-1/2} + \frac{eV_n\tau}{2\pi}(\sin\Phi_n - \sin\Phi_{s,n}) + \frac{e^2g_0}{4\pi\epsilon_0} \frac{h^2\tau}{R\gamma_{s,n}^2} \left(\frac{d\lambda(\Phi)}{d\Phi} \right)_n, \quad (1)$$

$$\Phi_{n+1} = \Phi_n + h\tau \left(\frac{\eta_s \omega_s^2 W}{\beta_s^2 E_s} \right)_{n+1/2} + \Phi_{s,n+1/2} - \Phi_{s,n-1/2}, \quad (2)$$

where the subscript n indicates that a quantity is evaluated at a time $t = n\tau$, τ = step-size, and the subscript s refers to a particle which, in the absence of space charge, remains on the equilibrium orbit (synchronous particle). We define

$$W_n = \frac{E_n - E_{s,n}}{\omega_{s,n}}, \quad (3)$$

with $\omega_{s,n}$ the synchronous angular frequency at $t = n\tau$. In Eqs.(2) and (3) Φ_n is the rf phase, g_0 is a geometrical factor

$$g_0 = 1 + 2ln(b/a), \quad (4)$$

where a is the beam radius and b is the radius of the vacuum chamber, λ is the linear particle density, V is the total rf gap voltage per turn, h is the harmonic number, and η is the dispersion factor.

*Work supported by U. S. Department of Energy, Office of Basic Energy Sciences under Contract No. W-31-109-ENG-38.

†Also Dept. of Physics, University of Wisconsin-Madison, Madison, WI 53706, USA

Table 1: Summary of tracking results for different initial conditions.

Case	Initial Bunch Length [deg]	Initial Energy Half-Spread [MeV]	Initial Bunch Area [eV-sec]	Bucket Area at \dot{B}_{max}	Peak Voltage [kV]	Dilution	Losses %
A1	180.0 (50% chopping)	1.0	0.7	3.0	110	3.3	0.0
A2		1.0	0.7	4.5	120	5.0	0.0
A3		1.5	1.1	4.5	120	3.3	0.0
A4		2.0	1.4	4.5	120	2.5	0.0
A5		2.5	1.8	4.5	120	2.0	0.0
B1	216.0	1.0	0.8	3.0	110	2.8	0.1
B2	(40%)	2.0	1.7	4.5	120	2.1	0.0
C1	240.0	1.0	0.9	4.5	120	3.8	0.0
C2	(34%)	2.0	1.9	4.5	120	1.9	0.2

The time-step is set to one turn during injection so that the injection process can be followed with maximum accuracy; during acceleration, the step-size can be increased optionally, to reduce computer time. (The time step must of course be kept much smaller than the synchrotron period or other relevant periods of the motion.)

Throughout the cycle we can "track-back" the initial coordinates of each particle, which is especially useful in determining the initial configuration of particles that are lost and in formulating different injection schemes.

Great care is taken in calculating the self fields as they influence considerably the particle distribution, reduce the bucket area, possibly distort the bucket shape, and degrade the capture efficiency. We are studying several methods of reducing the statistical fluctuations due to the relatively coarse ensemble of macro particles used in the simulations. For the tests summarized in this paper, the particle distribution is binned using the cloud-in-cell method. The cell grid is chosen fine enough to accommodate the structure of the bunch distribution, yet coarse enough to attenuate the short wavelength noise due to the finite number of macro particles. The data is then fast-Fourier transformed, padded with zeros to obtain a finer grid. The Fourier components are then multiplied by a Lanczos convergence factor. Tests have shown that a cut-off frequency at the 11th harmonic reduces noise with an acceptable underestimation of the peak and overestimation of the bunch ends, introduced by the filtering process. An optimal (Wiener) filter to produce the best estimate of the standard distribution from the computed distribution is also being investigated [3].

2.2 Testing the Tracking Program

We first checked the tracking program by verifying that it gives the correct stationary and moving bucket shapes in the absence of space charge forces.

In order to check that space charge forces are properly included, we ran the program above the transition energy with the rf voltage off and verified that the negative mass instability appears with the correct threshold and correct growth rate.

In order to provide us with guidance in choosing the rf

voltage schedule, we ran some self-consistent solutions for stationary and moving buckets in the presence of space charge. We start with an initial distribution of particles in phase space near the expected solution, and run the simulation until the distribution and space charge potential settle into a nearly stationary configuration. We then check that the orbits resulting from this space charge potential (plus the rf voltage) agree with the simulated orbits. An example result is shown in Figure 1.

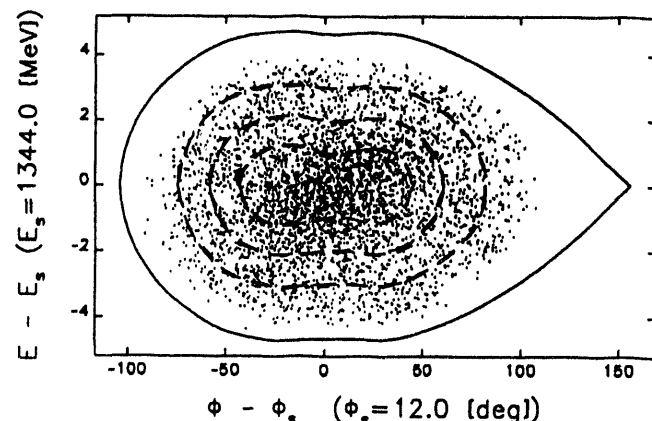


Figure 1: Phase space distribution of particles injected near a stationary distribution, after 40 synchrotron oscillations. The dashed lines represent Hamiltonian contours for this distribution.

3 SIMULATION

3.1 Results

In the present studies, we assume that the linac provides a beam pulse 0.5 msec in length (corresponding to 555 turns) and a pulse current big enough to accumulate 1.0×10^{14} protons per pulse. We assume also that the low energy chopper has a frequency equal to the revolution frequency and has a variable duty factor. Although the typical energy spread of the design linac is 0.5%, our simulations treat $\Delta T/T$ as a variable input parameter so we can assess its effects on beam losses and on the time-varying momentum spread, which plays an important role in beam instability considerations [4].

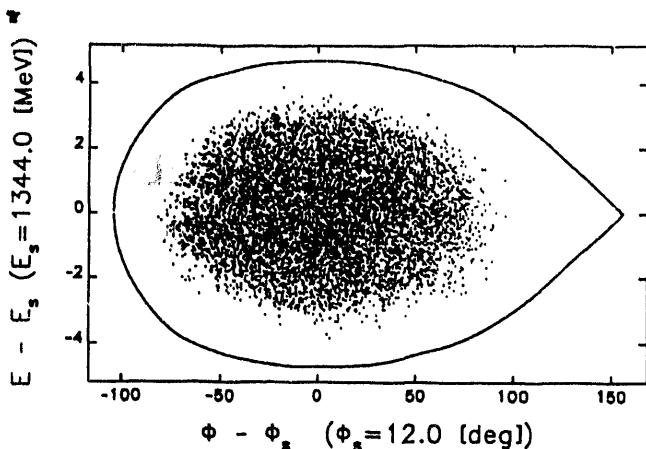


Figure 2: Phase space distribution after 1 msec of acceleration for Case A4.

We simulate the injection process by placing a beam of given length and energy spread into a waiting bucket in 555 turns, under a "flat bottom" regime ($\dot{B} = 0$), to facilitate injection manipulations. The beginning of the acceleration clock is set at the end of injection. Since the magnet system is energized with a biased sinusoidal wave form, the maximum rate of increase of magnetic field occurs at the halfway point of the accelerating period (12.5 msec). The corresponding maximum energy gain together with an assumed synchronous phase of 45° provide the peak voltage of the rf system (about 120 kVolts). We then calculate the bucket area at \dot{B}_{\max} , where it is at a minimum, and program the rf voltage during acceleration so as to maintain a constant bucket area.

In Table 1, we summarize the simulation results for nine cases with various injected bunch lengths and beam energy spreads and emittances at the end of injection. We tabulate the bucket area at \dot{B}_{\max} , the dilution, and the particle losses. The dilution parameter is computed as the ratio between the bucket area at its minimum and the initial beam area.

In the cases with a 4.5 eV-sec bucket area, the bucket height is greater than the energy spread required by preliminary calculations of the micro-instability threshold. In Figure 2 we show the phase space at a typical time for case A4. Case A4 is best matched to the 4.5 eV-sec bucket. Initial beams of 1 MeV half-energy spread and long lengths are badly matched to the bucket, resulting in strongly peaked space charge potentials with wide side shoulders (Cases B1 and C1). In both cases, loss of restoring force occurs at about 1 msec of acceleration. This can be seen in Figure 3, where the instantaneous total energy gain per turn has a negative slope for the particles near the synchronous phase. At that time, the bucket is noticeably depressed (see Figure 4). In Case C1 there are also large area oscillations during the cycle.

3.2 Future Plans

We are presently studying methods of increasing the bunch length and/or the energy spread as a means to insure microwave stability. One possibility is to add a second har-

monic to the rf voltage whose magnitude and phase displacement with respect to the fundamental optimizes the available bucket area.

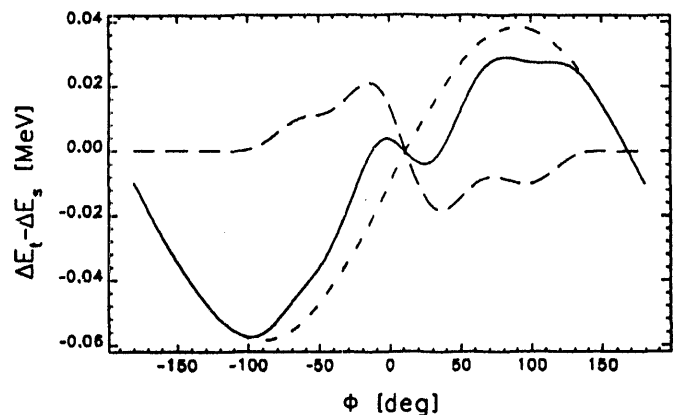


Figure 3: Instantaneous energy gain per turn after 1 msec of acceleration for Case C1. The solid line represents the total gain; the dashed line, the gain due to space charge forces; and the short-dashed, that due to the rf voltage.

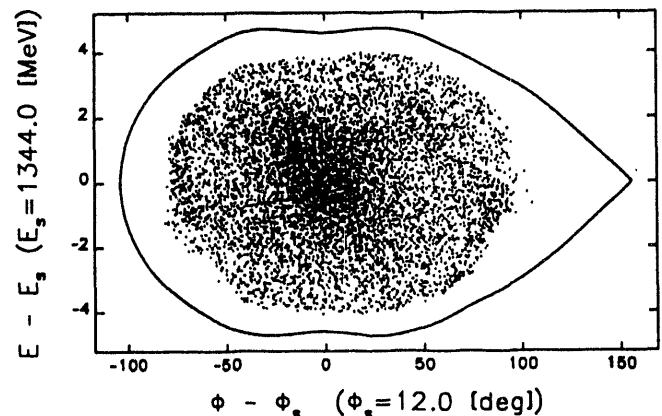


Figure 4: Phase space distribution after 1 msec of acceleration (Case C1).

4 REFERENCES

- [1] Y. Cho *et al*, "Conceptual Design for One Spallation Neutron Source at Argonne," *Particle Accelerator Conference*, 3757-3759 (1993).
- [2] K. R. Symon, "Synchrotron Motion with Space Charge," *NSA-94-3*(1994).¹
- [3] K. R. Symon, "Optimal Filtering in Space Charge Simulations," *NSA-94-4* (1994).¹
- [4] A. Hofmann, "Single-Beam Collective Phenomena - Longitudinal," *Proc. of Theoretical Aspects of the Behaviour of Beams in Accelerators and Storage Rings*, CERN 77-13 (1976).

¹This is a Neutron Source Accelerator report, available by request from the authors.

DISCLAIMER

This report was prepared as an account of work sponsored by an agency of the United States Government. Neither the United States Government nor any agency thereof, nor any of their employees, makes any warranty, express or implied, or assumes any legal liability or responsibility for the accuracy, completeness, or usefulness of any information, apparatus, product, or process disclosed, or represents that its use would not infringe privately owned rights. Reference herein to any specific commercial product, process, or service by trade name, trademark, manufacturer, or otherwise does not necessarily constitute or imply its endorsement, recommendation, or favoring by the United States Government or any agency thereof. The views and opinions of authors expressed herein do not necessarily state or reflect those of the United States Government or any agency thereof.

DATE

FILMED

8/24/94

END

